Vol. 47, No. 2 (2025) 187-201, DOI: 10.24874/ti.1868.01.25.03

Tribology in Industry

www.tribology.rs

RESEARCH

Green Composites for Future Applications: Investigating the Influence of CSP and GGBS on the Mechanical Properties of Bamboo-Jute-Sisal Natural Fiber Reinforced Hybrid Composites

H. Amitkumar[a], G. Mallesh[b,*]

[a]*Research Scholar, Department of Mechanical Engineering, Sri Jayachamarajendra College of Engineering, JSS STU, Mysuru, Karnataka, India,*
[b]*Professor, Department of Mechanical Engineering, Sri Jayachamarajendra College of Engineering, JSS STU, Mysuru, Karnataka, India.*

Keywords:

Green composites
Sisal jute and bamboo fibers
CSP and GGBS fillers
Hand layup and bag molding techniques
Mechanical properties
Application of green composites

* Corresponding author:

G. Mallesh
E-mail: mallesh@sjce.ac.in

Received: 12 January 2025
Revised: 21 February 2025
Accepted: 4 March 2025

A B S T R A C T

In recent years, natural fiber reinforced composites (NFRCs) have gained significant attention due to their potential to replace synthetic fibers in various applications. This research focuses on developing green composite materials by combining sisal, jute, and bamboo natural fibers with epoxy resin filled with Coconut Shell Powder (CSP) and Ground Granulated Blast Furnace Slag (GGBS). The composites were fabricated using hand layup and bag molding processes with varying fiber volume fractions of 5%, 10%, and 15%. The results showed that GGBS-filled composites exhibited superior tensile strength, flexural strength, and impact strength, with average tensile strength enhancements of 18.3% (Sisal), 19.9% (Jute), 15.3% (Bamboo), and 10.7% (Hybrid fibers). Additionally, GGBS-filled composites displayed higher Shore D hardness, with Bamboo-GGBS exhibiting a 14.45% higher hardness than Bamboo-CSP. Furthermore, water and oil absorption percentages were reduced by 24.5% (water) and 32.1% (oil) for Sisal, 22.1% (water) and 29.5% (oil) for Jute, 26.3% (water) and 34.1% (oil) for Bamboo, and 23.2% (water) and 30.5% (oil) for Hybrid. EDAX and SEM analyses confirmed the composition and microstructure of the developed NFRCs, revealing strong interfacial bonding, uniform filler distribution, and distinct energy levels of constituents. Overall, these NFRCs, made from Sisal, Jute, and bamboo fibers filled with CSP and GGBS, offer a durable and sustainable solution for various industries, including automotive, aerospace, medical devices, renewable energy, and construction.

1. INTRODUCTION

Composite materials are engineered by combining two or more distinct materials to create a strong, lightweight, and durable material. Natural fibers, including Sisal, Jute, and bamboo, have emerged as promising reinforcements in composite materials,

enhancing strength, stiffness, and sustainability. As eco-friendly alternatives to synthetic fibers, these natural fibers offer a sustainable solution for various applications, such as aerospace, automotive, sports equipment, and industrial components [1]. Natural fibers require specific extraction and treatment methods to optimize their performance and compatibility for various applications, including composite materials fabrication. Extraction methods vary by fiber type: sisal undergoes decortication, jute is retted using water or microbial methods, and bamboo is retted and then mechanically separated. Further treatment methods, such as water retting, alkaline solutions, and steam explosion (for bamboo), enhance fiber properties. Alkaline treatment, in particular, improves surface properties and compatibility with polymer matrices. These extraction and treatment methods are critical in determining the quality and performance of natural fibers for various applications [2,3]. Matrix materials play a crucial role in FRP composites, acting as a binding agent that ensures fiber cohesion and imparts structural integrity. Epoxy resins are widely preferred for FRP composites due to their outstanding mechanical properties, including high strength, adhesion, chemical resistance, dimensional stability, and minimal shrinkage during curing [4]. The rapid urbanization and industrialization of developing countries have led to a significant increase in solid waste generation and pollution. Asia, accounting for approximately 70% of global coconut cultivation, generates a substantial amount of waste from discarded coconut shells. Additionally, Ground Granulated Blast Furnace Slag (GGBS), a by-product of iron and steel production, is underutilized, with approximately 15% of the produced GGBS remaining unused. The burning of coconut shells and disposal of unused GGBS in landfills contribute to environmental pollution and waste management issues [5,6]. However, research offers a promising solution, as incorporating Coconut Shells Powder (CSP) and GGBS into FRP composites has been shown to improve their mechanical properties.

In this research, an effort is made to develop sustainable green composites by combining natural fibers with eco-friendly fillers. The study investigates the effect of varying volume fractions of fibers on the mechanical properties to exploring their potential applications.

2. LITERATURE REVIEW

The literature review focuses on the synthesis and mechanical characterization of Natural Fiber-Reinforced Composites (NFRCs), examining existing studies on the reinforcement of epoxy resin with jute, bamboo, and sisal fibers, as well as their combination with various fillers. Vijay et al. [7] investigated jute-epoxy FRP composites fabricated via hand layup with 0-12.5% fiber weight fractions. Results showed optimal tensile (54.06 MPa) and flexural (67.55 MPa) strengths at 5% fiber content, and superior viscoelastic properties at 7.5% fiber content. Flores et al. [8] examined the effects of hybridizing jute with glass and carbon fibers on mechanical properties. Hybrid composites showed 50-75% improved performance over pure glass and carbon composites, and 20-30% over pure jute composites. Sonali et al. [9] found that jute/E-glass composites outperformed others, with 10% jute fibers showing enhanced tensile strength and 40% jute/PLA achieving highest flexural strength. Senthil et al. [10] found that chemical treatment increased water absorption in hybrid composites, but optimizing PLA matrix compatibility with alkaline-treated jute fibers minimized water uptake. Xian et al. [11] found that adding Bamboo Pulp Fibers (BPF) to Bamboo Plastic Composites (BPCs) significantly enhanced flexural, tensile, and impact strength, highlighting bamboo fibers potential as a sustainable reinforcement material. Chin et al. [12] fabricated Bamboo Fiber-Reinforced Composites (BFRCs) with 40% fiber volume fraction, achieving optimal mechanical properties (tensile strength: 119.39 MPa, flexural strength: 161.58 MPa) and exceptional thermal stability. Xie et al. [13] found that Bamboo Fiber Composites (BFCs) with a density of 1200 kg/m^3 exhibited improved dimensional stability (water absorption: 5.01%, width swelling: 0.7%, thickness swelling: 5.5%) and superior mechanical properties (shear strength: 18.52 MPa, compressive strength: 159.75 MPa, modulus of elasticity: 240.99 MPa). Latha et al. [14] developed a bamboo-glass hybrid composite, achieving 80% of pure glass composite strength. The optimal GBBG hybrid laminate, with 20% glass fiber, exhibited tensile strength of 47.74 MPa and modulus of 5.4 GPa, as well as flexural strength of 161 MPa and modulus of 6.8 GPa. Huang et al. [15] developed bamboo fiber-reinforced epoxy composites using resin

transfer molding. Alkali-treated bamboo fibers significantly improved mechanical properties, achieving tensile strength of 222.71 MPa, Young's modulus of 13.10 GPa, flexural strength of 182.29 MPa, and flexural modulus of 17.23 GPa. However, moisture absorption negatively impacted mechanical properties, highlighting the need for further optimization. Liu et al. [16] developed a novel bamboo fiber extraction method and treated the fibers with IEM and DBTDL catalyst. This enhanced the mechanical properties of bamboo-UPE composites, achieving tensile strength of 42-66 MPa, flexural strength of 76-105 MPa, and flexural modulus of 5,300-6,800 MPa, while improving water resistance, although impact strength decreased to 15-19 kJ/m2. Zhihua et al. [17] found that optimal alkali treatment of sisal fibers improved their tensile strength and interfacial bonding with polylactic acid (PLA), with lignin playing a key role as a natural compatibilizer to enhance interfacial bonding. Vishnuvardhan et al. [18] investigated sisal fibre-reinforced epoxy composites with varying fibre-to-resin ratios, finding that tensile strength increased by 15% to 41.65 MPa, flexural strength increased by 18% to 81 MPa, and impact strength increased by 10% to 12.8 J at the optimal fibre content of 25% (S25), but water absorption also rose due to sisal fibre's hydrophilic nature. Li et al. [19] and Zhou et al. explored the potential of sisal fibre as a reinforcement in composites. They found that sisal fibre's mechanical and physical properties vary depending on source and experimental conditions, but fibre treatment improves adhesion and reduces water absorption. Additionally, optimizing cellulose, hemicellulose, and lignin content ratios through alkali treatment can enhance tensile strength and interfacial bonding with poly lactic acid (PLA) matrices, with crystallinity increasing linearly with hemicellulose content. Devaraju et al. [20] investigated the mechanical properties of sisal fiber composites with and without nanoparticles (NPs). Results showed that incorporating ZnO and ZrO2 NPs (0.5 wt.%) enhanced tensile strength, impact resistance, and Brinell hardness by up to 45%, but surprisingly did not improve flexural strength. Bekele et al. [21] treated sisal fibers with 5% and 10% NaOH solutions, finding that 5% NaOH treatment improved tensile strength and tenacity, while reducing moisture absorbance and fiber diameter, and slightly increasing fiber density.

Gudayu et al. [22] found that combining alkali treatment and acetylation improved sisal fiber's hydrophobicity, thermal stability (up to 300°C), and reduced thermal decomposition (by 30.9-49.6%), while maintaining mechanical strength, with a 17% reduction in fiber diameter (from 300 μm to 250 μm). This optimal combination method achieved a balance between improved properties, unlike acetylation alone which decreased tensile strength by 25%. The combined treatment also removed impurities, enhancing the overall quality of the sisal fiber. Khan et al. [23] explored heat-treated sisal fiber reinforced epoxy composite as a sustainable replacement for metallic leaf springs in electric vehicles, achieving tensile strengths of 65 MPa (unidirectional) and 53 MPa (woven), flexural strengths of 170 MPa (unidirectional) and 148 MPa (woven), and impact strengths of 13 MPa (unidirectional) and 14 MPa (woven). Finite element analysis confirmed its potential, with maximum deformation values of 59.77 mm (unidirectional) and 45.339 mm (woven), and von Mises stress values of 224.87 MPa (unidirectional) and 219.23 MPa (woven), making it a viable eco-friendly alternative. Moshi et al. [24] studied sisal-banana natural fiber composites with varying compositions. They found that adding banana fiber increased tensile strength (up to 31.68 MPa) but decreased flexural strength (to 46.61 MPa). The optimal composition was 25%S-10%B-65%E, as confirmed by experimental and numerical analysis using Ansys software. The literature review explores NFRCs, focusing on jute, bamboo, and sisal fibers. Studies investigated fiber treatment, content, and hybridization, yielding improved tensile strength, flexural strength, impact resistance, and thermal stability. Despite the potential of NFRCs, research on the hybridization of fibers and the effects of adding CSP and GGBS on mechanical and tribological properties is limited. This study aims to address this knowledge gap.

3. SYNTHESIS AND FABRICATION OF SUSTAINABLE NFRC'S

For this study, alkali-treated plain-woven fabrics of sisal, jute, and bamboo, sourced from Sri Lakshmi Group Exports and Imports in Guntur, Andhra Pradesh, India, were utilized to fabricate Natural Fiber-Reinforced Composites (NFRCs)

with varied fiber volume fractions. Building on existing research, it has been established that NFRCs with fiber volume fractions exceeding 30% and matrix volume fractions below 40% often exhibit inadequate bonding [25].

Therefore, to prevent debonding and delamination, the maximum fiber volume fraction was maintained at 30% in this study. Specifically, three different fiber volume fractions were initially considered: 10%, 20%, and 30%. The fabrics selected for NFRCs, along with their physical properties, are listed in Table 1 and illustrated in Fig. 1.

Table. 1. Properties of natural fibers.

Properties	Jute	Sisal	Bamboo
Tensile Strength, MPa	510-710	610-820	290
Young's modulus, GPa	26.5	9-22	17
Density (gcm^{-3})	1.40	1.34	1.25

Sisal Fabric mat Jute Fabric mat

Bamboo Fabric mat

Fig. 1. Sisal, jute and bamboo fabric mat.

The matrix plays a crucial role in Fiber-Reinforced Polymer (FRP) composites, binding fibers together and facilitating stress transfer, and its selection significantly influences the compressive, inter-laminar shear, and in-plane shear properties of FRP composites. Common matrices include epoxy, polyester, phenolic, and silicone resins, with epoxy resin being widely preferred due to its excellent adhesion, high strength, durability, and ease of processing.

Therefore, for this research work, a combination of Epoxy Resin (LY556 grade) and Hardener (HY951 grade) in a 12:1 weight ratio was selected owing to its exceptional mechanical integrity, thermal stability, low shrinkage, and excellent adhesive properties, all achieved at a relatively low cost [26]. The properties of the epoxy resin and hardener are summarized in Table 2.

Table. 2. Properties of resin and hardener.

Properties	Epoxy LY556	Hardener HY951
Viscosity (mPas)	120–130	10-20
Density (gcm^{-3})	1.1-1.2	0.946

Adding fillers to a polymer matrix in composite materials serves to reduce cost, enhance modulus, minimize mold shrinkage, and regulate viscosity for a smooth surface finish. To mitigate environmental pollution and waste management issues, CSP and GGBS fillers are incorporated into FRP composites, enhancing their mechanical properties. EDAX analysis was performed on CSP and GGBS to determine the presence of particles. The results, shown in Fig. 2 and 3, reveal that SiO_2, SiC, Al_2O_3, $MgCO_3$, $CaCO_3$, and $CaCl_2$ are present in both CSP and GGBS exhibiting distinct energy peaks in the K and L shells. In conclusion, this study fabricated NFRCs using Sisal, Jute, and Bamboo fibers, epoxy resin, CSP and GGBS fillers. The mechanical properties of these NFRCs were evaluated by varying the volume fraction of fibers, matrix, and fillers.

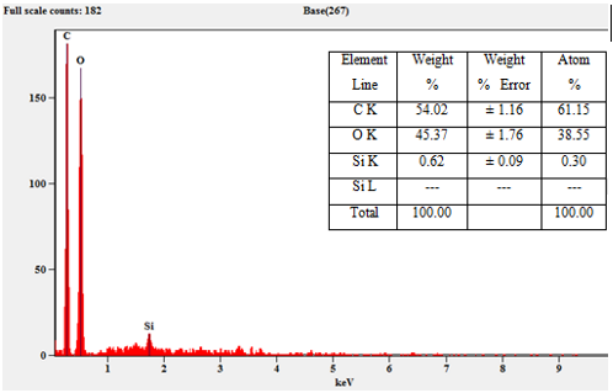

Fig. 2. EDS spectrum of GGBS.

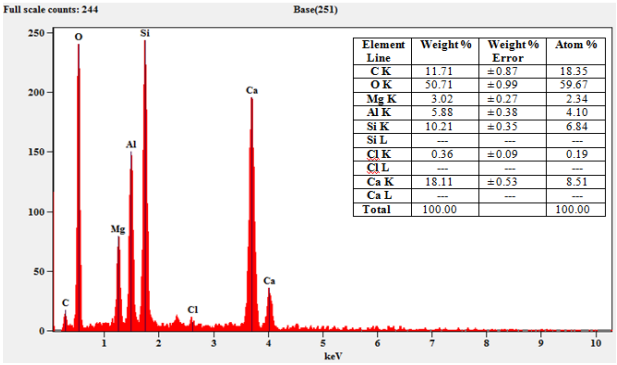

Fig. 3. EDS spectrum of GGBS.

A composite sheet with dimensions (400 x 400 x 3) mm was fabricated using hand layup and bag molding processes. The volume fractions of various samples are summarized in Table 3. To calculate the mass of each constituent, their densities and volume fractions were used in Equation 1. The computed masses for samples containing a 10% volume fraction of fibers are presented in Table 4.

$$Mass(g)=Density(\rho)\times Volume\ fraction\ (V_c) \quad (1)$$

Table. 3. Materials and their volume fractions in Fabrication of NFRCs filled with CSP and GGBS.

Materials	Volume Fraction											
	Sisal			Jute			Bamboo			Hybrid		
	S_1	S_2	S_3	J_1	J_2	J_3	B_1	B_2	B_3	H_1	H_2	H_3
Fibers	10	20	30	10	20	30	10	20	30	15	22.5	30
Matrix	80	65	50	80	65	50	80	65	50	75	62.5	50
CSP	10	15	20	10	15	20	10	15	20	10	15	20
GGBS	10	15	20	10	15	20	10	15	20	10	15	20

Table. 4. Mass of fiber, matrix and fillers for samples (S_1, J_1 & B_1).

Materials		Density (gcm^{-3})	Volume Fraction	Mass (g)
Fiber	Sisal	1.5	10	72
	Jute	1.3	10	62.4
	Bamboo	1.1	10	52.8
Matrix	Epoxy Resin	1.56	80	599.04
Fillers	CSP	1.6	10	76.8
	GGBS	2.8	10	134.4

Fig. 4. Fabrication stages.

The fabrication process of the NFRC laminate involves several steps, as illustrated in Fig. 4. First, the required number of layers of sisal, jute, and bamboo fabric mat strands are marked and cut to the specified dimensions using a marker and scissors. The number of layers is determined by the desired thickness of the laminate. Next, the matrix preparation involves mixing a predetermined quantity of matrix resin with the hardener, followed by blending with the filler.

The layer application process entails positioning the initial layer of sisal, jute, or bamboo fibers on a cleaned, flat surface. A resin layer is then applied using a spray gun or brush, and this process is repeated until the desired thickness is attained. To remove excess resin, perforated and breather sheets are placed on the surface. Finally, the laminate undergoes vacuum consolidation for 1 hour and 30 minutes to eliminate air bubbles and excess resin.

The initial curing process involves curing the composite for 1 hour at 100°C, maintaining vacuum pressure to optimize air bubble and excess resin removal. Following this, the laminates undergo post-curing in a hot air oven for 24 hours at 80°C, as illustrated in Fig. 5, which enhances the material properties, strength, durability, and overall performance of the NFRCs.

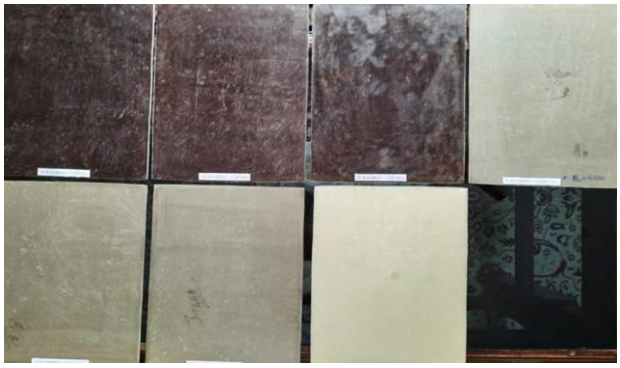

Fig. 5. Sisal/jute/bamboo/hybrid laminates.

Post-cured laminates were marked and cut into test specimens using a water jet machine, in accordance with ASTM standards, as shown in Fig. 6.

These specimens were then evaluated for their mechanical properties, including tensile strength, flexural strength, impact resistance, interlaminar shear strength (ILSS), and hardness. In addition, water and oil absorption tests were conducted to assess their performance under various environmental conditions.

Fig. 6. Specimen preparation stages.

4. EVALUATION OF MECHANICAL AND PHYSICAL PROPERTIES OF NFRCS

Mechanical and physical characterization of NFRCs was performed through a series of tests. Tensile tests were conducted according to ASTM D3039 using an INSTRON H10KS machine at a crosshead speed of 1.0 mm/min. Load-displacement data was recorded until failure.

Flexural testing was performed using the 3-point bending test method (ASTM D790-03) on a computerized universal testing machine at a crosshead speed of 0.5 mm/min. This test determined the flexural strength and stiffness of NFRCs with varying fiber volume fractions.

Interlaminar shear strength (ILSS) was evaluated using a standardized three-point flexure test on short beam specimens (90 x 13 x 3.2 mm) according to ASTM D2344. The test involved setting up the specimen on support rollers, aligning it centrally, and applying force at 5 mm/min using a UTM, with a maximum travel distance of 12 mm.

Impact testing was conducted according to ASTM D-256 standard Izod impact tests to evaluate the impact strength of NFRCs. Hardness testing was performed using a Shore-D hardness tester in accordance with ASTM D-2240, with average values recorded from multiple locations on each specimen.

Density testing was conducted using a Mettler Toledo density tester according to ASTM D-792-86, and calculated using Equation 2. Water and oil absorption tests were conducted on NFRCs according to ASTM D570. For the oil absorption test, SAE 30 grade oil was used, and absorption percentages were calculated using Equation 3. Each test was conducted in triplicate for each volume fraction, and average values were calculated for the following properties: tensile strength, flexural strength, ILSS, impact strength, hardness, density, water absorption, and oil absorption.

Scanning Electron Microscopy (SEM) is a vital analytical tool for characterizing materials composition, structure, performance, and degradation. It plays a crucial role in quality control, material development, performance optimization, and failure analysis, ultimately enabling the development of safer and more effective materials. In this study, SEM was employed to investigate NFRCs, focusing on the distribution of reinforcement particles, surface morphology, and failure characteristics.

The ASTM standards and test specimen configurations used for these tests are illustrated in Fig. 7.

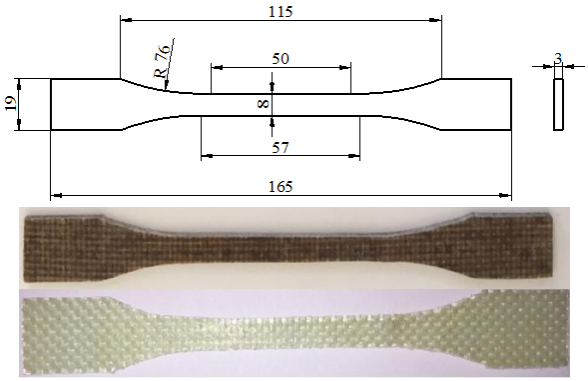

ASTM D3039 Tensile Test Specimen

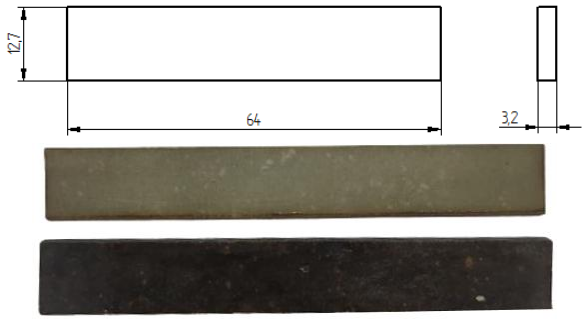

ASTM D790-03 & ASTM D-256 Impact/Flexural Test Specimen

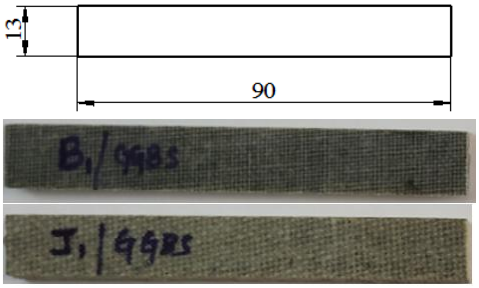

ASTM D2344 ILSS Test Specimen

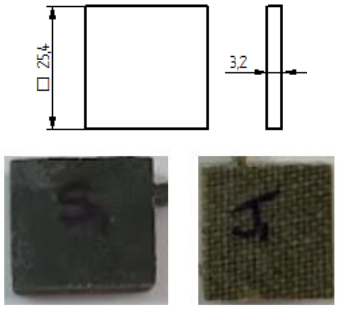

ASTM D-2240, ASTM D-792-86 & ASTM D570 Hardness, density, water and oil abruption Test Specimen

Fig. 7. ASTM test standards and specimen configurations.

$$\textbf{Density} = \left(\frac{Wt.in\ air\ (W_1)}{Wt.in\ air\ (W_1) - Wt.in\ water\ (W_2)}\right) Density\ of\ the\ std.liquid \quad (2)$$

$$\%\ \textbf{of absorption} = \left(\frac{Final\ wt.\ after\ immersion\ (W_2) - Initial\ wt.of\ dry\ Specimen(W_1)}{Initial\ wt.of\ dry\ Specimen(W_1)}\right) 100 \quad (3)$$

5. RESULTS AND DISCUSSIONS

The mechanical and physical properties of NFRCs filled with CSP and GGBS were investigated to assess the effects of fiber type, filler content, and fiber-filler interactions.

5.1 Tensile Properties of NFRCs

Table 5 compares the mechanical properties of CSP- and GGBS-filled composites. The results indicate that GGBS-filled composites exhibit slightly higher yield strength (20466.81-25023.79 N) and ultimate modulus (488.52-1009.58 MPa) than CSP-filled composites (20188.81-24776.03 N and 483.69-999.58 MPa, respectively). Moreover, GGBS-filled NFRCs demonstrate superior tensile strength across all fiber types, with average enhancements of 18.3% (Sisal), 19.9% (Jute), 15.3% (Bamboo), and 10.7% (Hybrid fibers). Notably, bamboo fiber composites exhibit exceptional tensile strength, while hybrid fiber composites show consistent improvements with GGBS filling. Although GGBS-filled composites exhibit superior tensile strength, CSP-filled composites display higher percentage elongation, ranging from 8.56% to 21.2%, compared to 7.70% to 19.08% for GGBS-filled composites. The differences in mechanical properties between CSP- and GGBS-filled composites are relatively minor, suggesting that both fillers can effectively reinforce the composites. The superior tensile strength of GGBS-filled FRP composites is attributed to favourable aspect ratios, interfacial bonding, and dispersion. In contrast, CSP-filled composites are hindered by lower aspect ratios and poor interfacial bonding. Additionally, fiber orientation, fiber-matrix adhesion, and epoxy matrix properties contribute to the enhanced tensile strength. This study reveals that bamboo composites exhibit the highest ductility among CSP-filled composites, while sisal composites show improved ductility with GGBS filling [27, 28].

Table. 5. Strength and deformation characteristics of NFRCs.

Sample	CSP Filled				GGBS Filled			
	Yield Strength, N	Ultimate modulus, MPa	% Elongation	Tensile Strength	Yield Strength, N	Ultimate modulus, MPa	% Elongation	Tensile Strength
S_1	20264.17	1022.41	8.56	63.98	20466.81	1032.63	7.704	87.26
S_2	22207.64	483.68	21.2	72.80	22429.71	488.52	19.08	91.24
S_3	22571.61	540.28	13.47	79.37	22797.32	545.68	12.12	95.52
J_1	21385.49	899.62	11.45	65.47	21599.34	908.62	10.31	80.63
J_2	20188.80	845.08	12.76	71.12	20390.69	853.53	11.48	83.16
J_3	22298.42	620.37	13.24	75.36	22521.41	626.58	11.92	90.11
B_1	23761.66	999.58	12.73	80.43	23999.27	1009.57	11.45	95.52
B_2	22432.01	938.98	14.18	86.17	22656.33	948.37	12.76	97.43
B_3	24776.03	689.31	14.72	92.96	25023.79	696.20	13.24	105.91
H_1	21559.23	528.77	10.06	80.70	21774.82	534.06	9.054	90.34
H_2	22261.11	807.61	11.7	86.33	22483.72	815.68	10.53	94.29
H_3	23745.19	777.88	15.13	90.64	23982.64	785.66	13.61	100.69

5.2 Flexural strength of NFRCs

Flexural testing is crucial for evaluating fiber-matrix bonding, ensuring the safety and reliability of composites. The assessment of interfacial bonding between fibers and matrix significantly impacts composite performance. Fig. 8 illustrates the flexural strength of NFRCs filled with CSP and GGBS. The results reveal substantial improvements with GGBS filling, with flexural strength increases of 27.4% (Sisal), 23.1% (Jute), 11.3% (Bamboo), and 12.1% (Hybrid) composites. These enhancements are attributed to enhanced interfacial bonding,

increased fiber-matrix interaction, and optimized fiber orientation. Furthermore, CSP and GGBS filling reduces voids and porosity, yielding denser composite with improved flexural strength. Notably, flexural strength increases with rising fiber volume percentage, a consistent trend across all composites with both GGBS and CSP fillings.

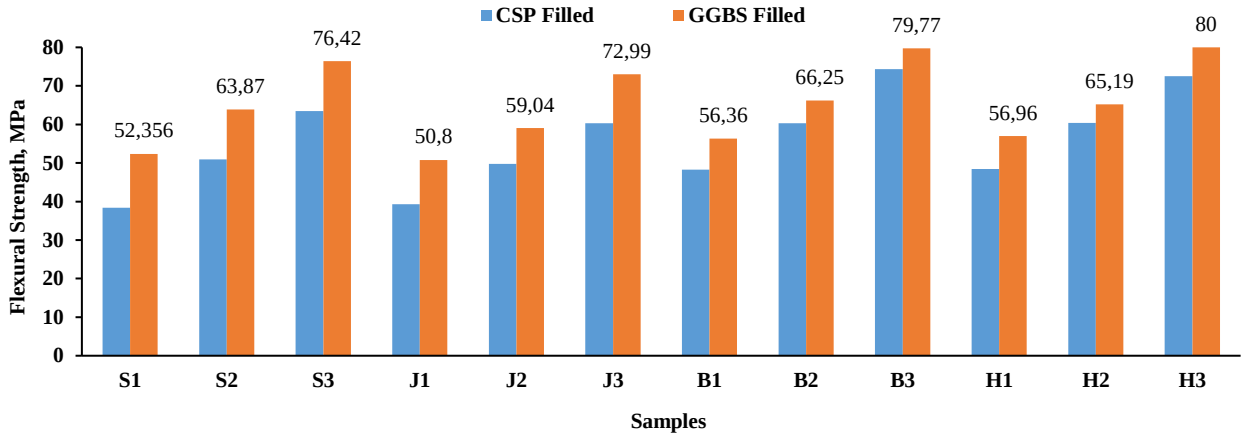

Fig. 8. Flexural strength of NFRCs.

5.3 Inter Laminar Shear Strength (ILSS) of NFRCs

ILSS evaluates critical composite performance aspects, including fiber-matrix interaction, load transfer, delamination resistance, and predictive behavior. Table 6 shows the ILSS values for NFRCs, revealing a significant increase in ILSS with rising fiber volume. Specifically, a 10% to 30% increase in reinforcement weight percentage yields notable enhancements: 39% for Sisal, 55% for Jute, 63% for Bamboo, and 72% for hybrid composites.

Table. 6. ILLS of NFRCs

Samples	ILSS, N/mm²	
	CSP Filled	GGBS Filled
S_1	22.49	29.23
S_2	28.59	37.17
S_3	31.41	40.84
J_1	11.46	14.1
J_2	12.94	15.92
J_3	20.68	25.44
B_1	11.87	14.12
B_2	14.01	16.67
B_3	18.98	22.59
H_1	25.86	34.14
H_2	32.88	43.4
H_3	36.13	47.69

The addition of CSP and GGBS fillers significantly improves ILSS due to enhanced interfacial bonding, chemical bonding, mechanical interlocking, reduced fiber agglomeration, and improved composite densification [28-30]. The hybrid effect of combining CSP and GGBS with natural fibers synergistically enhances ILSS, increasing resistance to delamination and interlaminar shear failure [30,31].

5.4 Impact Strength of NFRC's

Impact energy calculation is vital for assessing structural integrity and informing safety considerations, as it reveals the energy absorption capacity. Fig. 9 shows the impact energy absorption of Sisal, Jute, Bamboo, and hybrid composites NFRCs. The results indicate that impact energy increases proportionally with fiber loading volume. The addition of GGBS and CSP boosts impact energy by up to 17.6% across all samples, with Bamboo composites attaining the highest values. The improved impact strength of GGBS and CSP-filled composites results from effective filling of micro-gaps, enhanced interfacial bonding, reduced fiber agglomeration, and increased densification [31,32]. Replacing CSP with GGBS enhances impact strength by 17.1% (Sisal), 20.8% (Jute), 23.5% (Bamboo), and 14.5% (Hybrid). The improved impact strength is attributed to effective filling of micro-gaps, enhanced interfacial bonding, and increased densification [32-34].

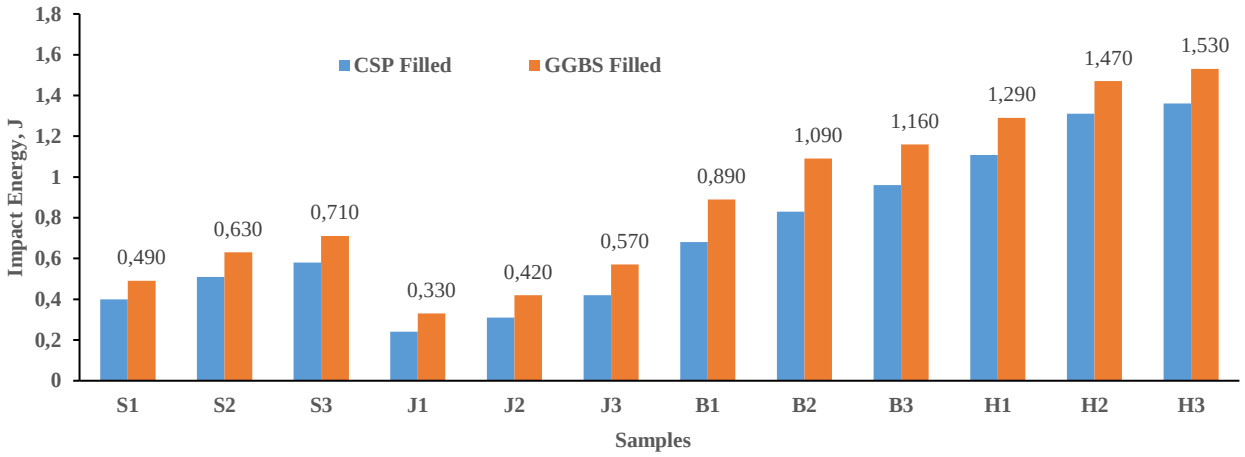

Fig. 9. Impact energy of NFRCs.

5.5 Shore D hardness of NFRC's

Table 7 presents the Shore-D hardness numbers for NFRCs, showing that Bamboo-CSP exhibits the highest hardness, followed by Hybrid-CSP, Sisal-CSP, and Jute-CSP. Notably, Sisal-CSP displays a 7.93% higher hardness than Jute-CSP, indicating superior hardness properties of Sisal fiber-reinforced composites compared to Jute-based composites. Similarly, among GGBS-filled NFRCs, Bamboo-GGBS exhibits the highest hardness, followed by Hybrid-GGBS, Sisal-GGBS, and Jute-GGBS, with Sisal-GGBS showing an 8.33% higher hardness than Jute-GGBS. A comparative analysis reveals that GGBS-filled NFRCs consistently exhibit higher hardness values than CSP-filled NFRCs across all fiber types, with Bamboo-GGBS and Hybrid-GGBS displaying 14.45% and 12.85% higher hardness than their CSP-filled counterparts, respectively. The improved hardness of GGBS-filled NFRCs is attributed to the finer particles, higher reactivity, and calcium-silicate-hydrate (C-S-H) gel formation of GGBS, which enhance interfacial bonding, fiber-matrix adhesion, and mechanical properties, while reducing porosity and fiber degradation [34,35]

5.6 Densities of NFRC's

The densities of NFRCs were measured using a Mettler Toledo density tester, and the results are presented in Table 8. A comparative analysis reveals that GGBS-filled composites consistently exhibit higher densities, with an average increase of 12.5%, than their CSP-filled counterparts across all fiber types. Sisal fiber composites displayed the highest density values, ranging from 1.256 to 1.592 g/cm^3, while Jute and Bamboo composites showed relatively lower densities. Statistical analysis indicates that GGBS-filled composites have a higher mean density (1.423 g/cm^3) and lower standard deviation (0.079 g/cm^3) compared to CSP-filled composites (1.243 g/cm^3, 0.084 g/cm^3). The enhanced density of GGBS-filled composites suggests improved fiber-matrix interaction and reduced porosity, making GGBS a more effective filler for natural fiber composites requiring higher structural integrity and durability [35,36]. Furthermore, the experimental density values of CSP and GGBS-filled composites were compared to theoretical models, including the Rule of Mixtures (ROM) and Halpin-Tsai model. The results showed that ROM predictions were lower than experimental values, whereas Halpin-Tsai model predictions were closer.

Table. 7. Shore D hardness number of NFRCs.

Samples	Shore D hardness Number	
	CSP Filled	GGBS Filled
S_1	62	68
S_2	65	73
S_3	68	78
J_1	53	58
J_2	58	66
J_3	63	72
B_1	79	87
B_2	81	92
B_3	83	95
H_1	67	74
H_2	68	77
H_3	70	81

Table. 8. Densities of NFRCs.

Samples	Density g/cm³	
	CSP Filled	GGBS Filled
S_1	1.256	1.413
S_2	1.364	1.502
S_3	1.497	1.592
J_1	1.163	1.358
J_2	1.287	1.467
J_3	1.384	1.564
B_1	1.149	1.278
B_2	1.241	1.361
B_3	1.368	1.489
H_1	1.227	1.379
H_2	1.338	1.436
H_3	1.429	1.565

5.7 Water and oil absorption behaviour of NFRCs

Tables 9 and 10 present the water and oil absorption behaviour of CSP and GGBS-filled NFRCs, respectively. Notably, oil absorption exceeds water absorption across all fiber combinations, due to the inherent properties of water and oil molecules. Specifically, water molecules face limited penetration due to hydrogen bonding and the hydrophilic-hydrophobic nature of the fiber-matrix interface, whereas oil molecules easily penetrate and fill voids. The results reveal that GGBS-filled composites consistently exhibit lower water and oil absorption percentages compared to CSP-filled counterparts across all fiber types. Specifically, GGBS-filled composites show average reductions of 24.5% (water) and 32.1% (oil) for Sisal, 22.1% (water) and 29.5% (oil) for Jute, 26.3% (water) and 34.1% (oil) for Bamboo, and 23.2% (water) and 30.5% (oil) for Hybrid fibers.

Table. 9. Water absorption % of NFRCs

Sample	% of Water Absorption	
	CSP Filled	GGBS Filled
S_1	4.239	3.189
S_2	4.468	3.200
S_3	4.765	3.541
J_1	5.131	4.013
J_2	5.426	4.294
J_3	5.738	4.511
B_1	3.814	2.899
B_2	4.191	3.133
B_3	4.241	3.196
H_1	4.546	3.492
H_2	4.739	3.621
H_3	5.043	3.861

Table. 10. Oil absorption % of NFRCs.

Sample	% of Oil Absorption	
	CSP Filled	GGBS Filled
S_1	11.231	7.614
S_2	11.615	8.431
S_3	12.615	9.372
J_1	12.698	8.674
J_2	13.923	9.146
J_3	15.651	9.823
B_1	8.285	6.272
B_2	8.621	6.866
B_3	9.874	7.478
H_1	11.093	8.411
H_2	12.196	8.731
H_3	13.761	9.063

This enhanced resistance to water and oil absorption stems from improved fiber-matrix adhesion, reduced porosity, uniform particle dispersion, and the inherent hydrophobicity of GGBS, making it a superior filler to CSP for natural fiber composites requiring improved durability and moisture resistance.

5.8 EDAX and SEM Analyses of NFRC's

SEM and EDAX (Energy-Dispersive X-ray Analysis) are crucial characterization tools for composite materials, enabling quality control, material development, performance optimization, and failure analysis. This facilitates the production of safer and more effective composite material systems. In this study, EDAX analysis was conducted on hybrid composites containing 20% volume fractions of CSP and GGBS fillers. Fig's 10 (a-f) present the EDAX spectra of hybrid NFRCs filled with CSP and GGBS, confirming the presence of each constituent at specific points and energy levels. The hybrid Sisal/Jute/Bamboo composites filled with CSP and GGBS demonstrated enhanced mechanical properties, which are attributed to the hard carbon particle content of 25-26% and 38-46%, respectively. Consequently, CSP and GGBS-based NFRCs offer a promising, cost-effective, environmentally sustainable, and regulatory-compliant alternative material solution for various engineering applications [36,37].

SEM imaging is a critical tool for elucidating material architecture, providing pivotal insights into surface properties, topography,

morphology, and microstructural features [37]. Through detailed micrographs, SEM analysis reveals key information on fiber distribution, filler dispersion, and matrix-fiber interactions. Fig's 11 (a-f) present SEM images of hybrid NFRCs filled with CSP and GGBS. A thorough examination of these images reveals several key features. Notably, the images display varying degrees of fiber alignment and distribution within the matrix, indicating differences in fiber orientation. Strong interfacial bonding between fibers and matrix is observed, with excellent adhesion evident in some areas. The fillers, CSP and GGBS, are generally well-distributed throughout the matrix, although some agglomerations are apparent. The surface topography and morphology vary, exhibiting roughness, porosity, and distinct fiber-matrix interfaces. Furthermore, microstructural features such as porosity, cracks, and fiber-matrix debonding are observed in all samples.

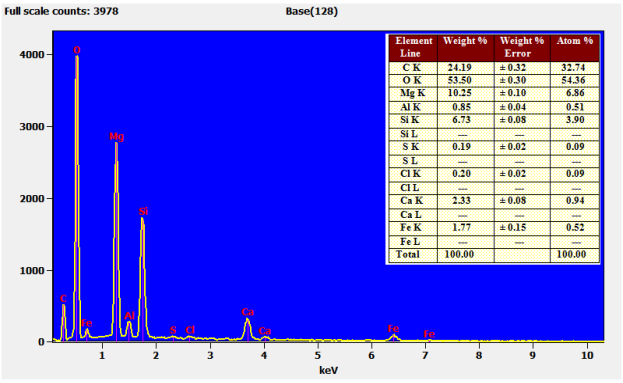

(a) Hybrid NFRCs (H1) filled with CSP

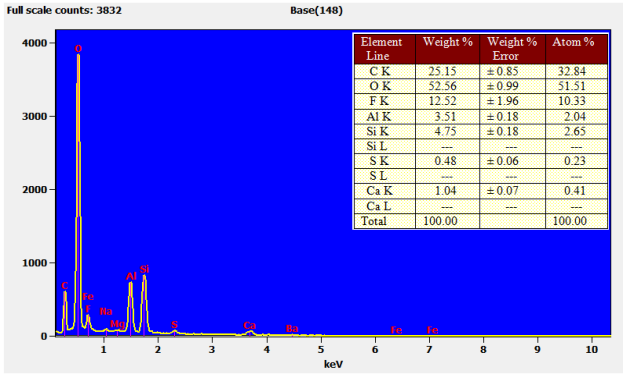

(b) Hybrid NFRCs (H2) filled with CSP

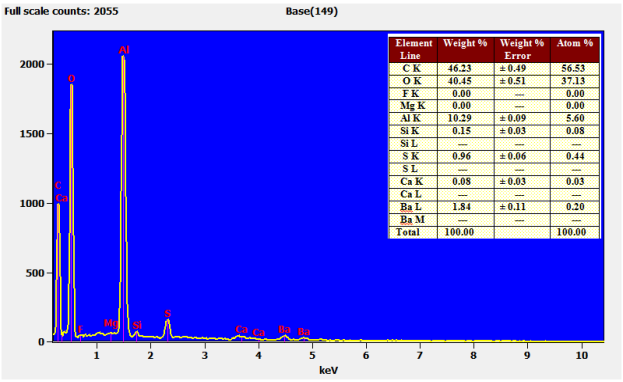

(c) Hybrid NFRCs (H3) filled with CSP

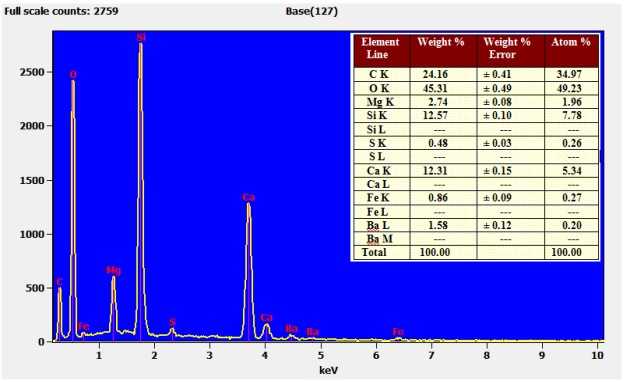

(d) Hybrid NFRCs (H1) filled with GGBS

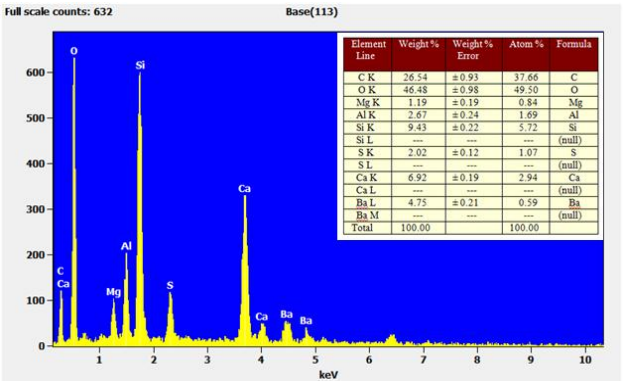

(e) Hybrid NFRCs (H2) filled with GGBS

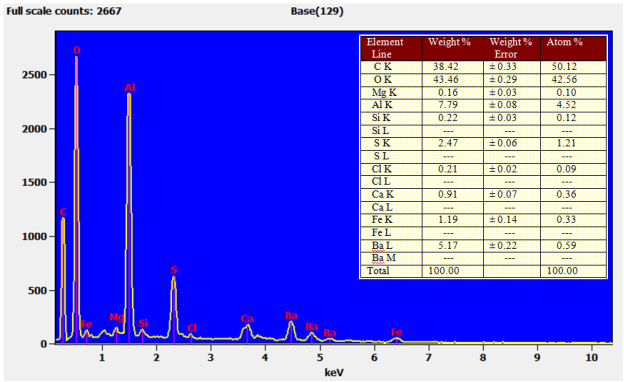

(f) Hybrid NFRCs (H3) filled with GGBS

Fig. 10. EDS Spectrum of hybrid NFRCs filled with CSP and GGBS.

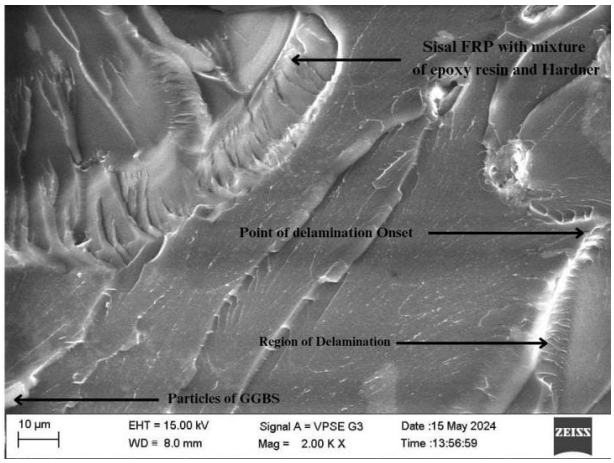

(a) SEM Micrographs of Hybrid NFRCs (H1) filled with CSP

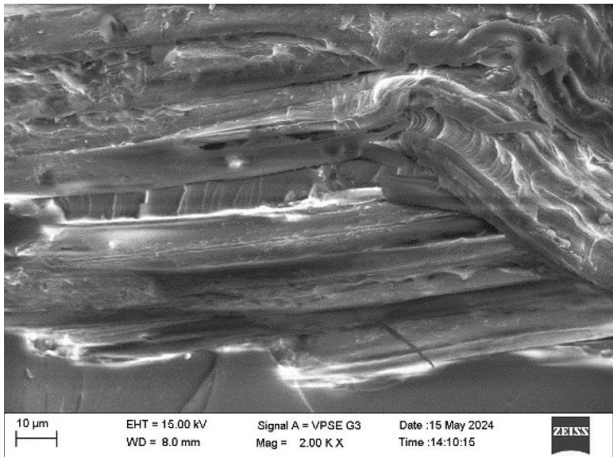

(b) SEM Micrographs of Hybrid NFRCs (H2) filled with CSP

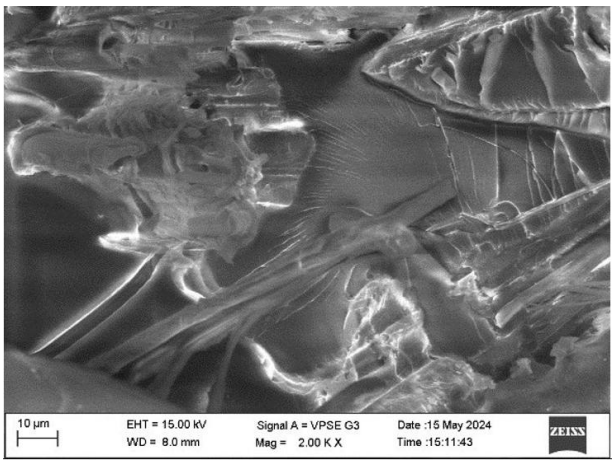

(c) SEM Micrographs of Hybrid NFRCs (H3) filled with CSP

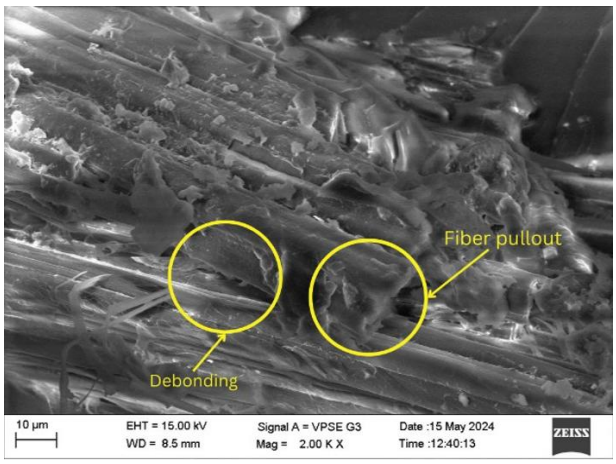

(d) SEM Micrographs of Hybrid NFRCs (H1) filled with GGBS

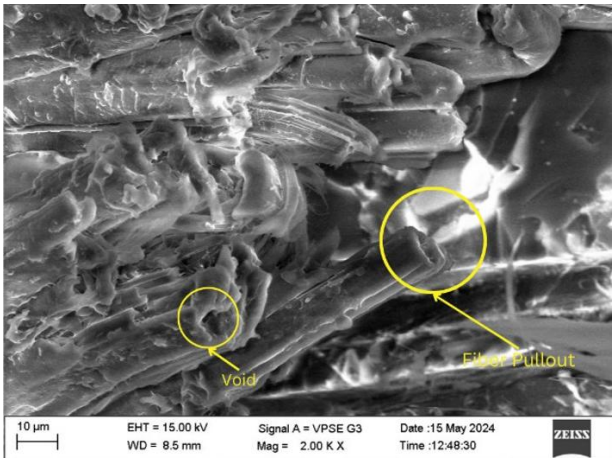

(e) SEM Micrographs of Hybrid NFRCs (H2) filled with GGBS

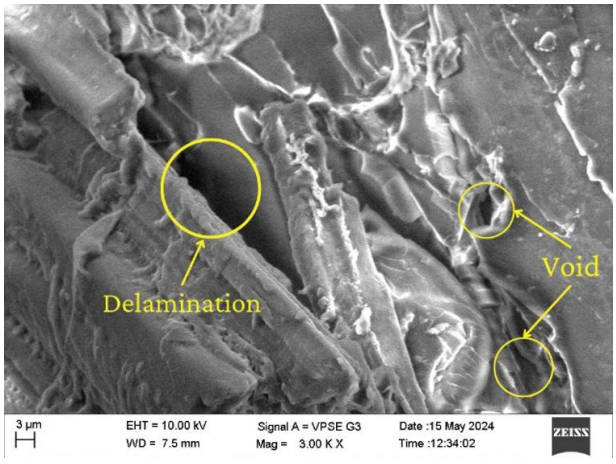

(f) SEM Micrographs of Hybrid NFRCs (H3) filled with GGBS

Fig. 11. SEM micro graphs of hybrid NFRCs filled with CSP and GGBS.

6. CONCLUSION

This study revealed significant enhancements in the mechanical and physical properties of natural fiber-reinforced composites (NFRCs) filled with Ground Granulated Blast Furnace Slag (GGBS) compared to Coconut Shell Powder (CSP). The incorporation of GGBS resulted in average tensile strength enhancements of 18.3% (Sisal), 19.9% (Jute), 15.3% (Bamboo), and 10.7% (Hybrid), as well as significant improvements in flexural strength, with increases of up to 27.4% (Sisal), 23.1% (Jute),11.3% (Bamboo), and 12.1% (Hybrid). Additionally, GGBS-filled composites

exhibited higher densities (average increase of 12.5%) and hardness values (improvements ranging from 12.85% to 14.45%) compared to CSP-filled composites. The study also found that GGBS-filled composites achieved average reductions of 24.5% in water absorption and 32.1% in oil absorption compared to CSP-filled composites. Microstructural analysis using EDAX and SEM confirmed the presence of all constituents and revealed enhancements in mechanical properties, thermal stability, and wear resistance, as well as strong interfacial bonding and well-distributed fillers throughout the matrix.

REFERENCES

[1] D. R. H. Jones and M. F. Ashby, *Engineering Materials 1: An Introduction to Properties, Applications and Design*, Butterworth-Heinemann, 2019.

[2] G. Bousfield, S. Morin, N. Jacquet, and A. Richel, "Extraction and refinement of agricultural plant fibers for composites manufacturing," *Comptes Rendus Chimie,* vol. 21, no. 9, pp. 897–906, Jul. 2018, doi: 10.1016/j.crci.2018.07.001.

[3] N. Chand and M. Fahim, *Natural fibers and their composites*, New Delhi, Periodical Experts Book Agency, 1994.

[4] J. C. Capricho, B. Fox, and N. Hameed, "Multifunctionality in epoxy resins," *Polymer Reviews*, vol. 60, no. 1, pp. 1–41, Aug. 2019, doi: 10.1080/15583724.2019.1650063.

[5] M. G. D. Abeysekara and K. P. Waidyarathne, "The Coconut Industry: A review of price forecasting modelling in major coconut producing countries," *CORD*, vol. 36, pp. 6–15, Nov. 2020, doi: 10.37833/cord.v36i.422.

[6] E. Basson, World Steel Association, "Key points from this report," 2020. [Online]. Available: (2020-World-Steel-in-Figures.pdf). [Accessed: *5 May 2024*].

[7] V. K. Mahakur, S. Bhowmik, P. K. Patowari, and S. Kumar, "Effect of alkaline treatment on physical, mechanical, and thermal characteristics of jute filler reinforced epoxy composites," *Journal of Vinyl and Additive Technology*, vol. 29, no. 2, pp. 330–342, Nov. 2022, doi: 10.1002/vnl.21963.

[8] A. Flores, A. Albertin, R. De Avila Delucis, and S. C. Amico, "Mechanical and hygroscopic characteristics of unidirectional Jute/Glass and Jute/Carbon hybrid laminates," *Journal of Natural Fibers*, vol. 20, no. 1, Mar. 2023, doi: 10.1080/15440478.2023.2178586.

[9] N. S. Sonali, N. M. Farzana, N. Md. M. Haque, N. A. Saha, N. R. A. Khan, and N. M. Mollah, "Natural fiber reinforced polymer-based composites: importance of jute fiber," *GSC Advanced Research and Reviews*, vol. 15, no. 1, pp. 021–029, Apr. 2023, doi: 10.30574/gscarr.2023.15.1.0078.

[10] J. Senthil, C. Thiagarajan, A. P. Sunil, N. A. T. S, and N. A. T. K, "Analysis on water absorption characteristics of chemically treated and untreated jute fiber/coconut husk particle reinforced hybrid bio-composites," *AIP Conference Proceedings*, vol. 2613, p. 020144, Jan. 2023, doi: 10.1063/5.0110708.

[11] Y. Xian, D. Ma, C. Wang, G. Wang, L. Smith, and H. Cheng, "Characterization and research on mechanical properties of bamboo plastic composites," *Polymers*, vol. 10, no. 8, p. 814, Jul. 2018, doi: 10.3390/polym10080814.

[12] S. C. Chin, K. F. Tee, F. S. Tong, H. R. Ong, and J. Gimbun, "Thermal and mechanical properties of bamboo fiber reinforced composites," *Materials Today Communications*, vol. 23, p. 100876, Dec. 2019, doi: 10.1016/j.mtcomm.2019.100876.

[13] J. Xie, J. Qi, T. Hu, C. F. De Hoop, C. Y. Hse, and T. F. Shupe, "Effect of fabricated density and bamboo species on physical–mechanical properties of bamboo fiber bundle reinforced composites," *Journal of Materials Science*, vol. 51, no. 16, pp. 7480–7490, May 2016, doi: 10.1007/s10853-016-0024-3.

[14] P. S. Latha, M. V. Rao, V. K. Kumar, G. Raghavendra, S. Ojha, and R. Inala, "Evaluation of mechanical and tribological properties of bamboo–glass hybrid fiber reinforced polymer composite," *Journal of Industrial Textiles*, vol. 46, no. 1, pp. 3–18, Feb. 2015, doi: 10.1177/1528083715569376.

[15] J.-K. Huang and W.-B. Young, "The mechanical, hygral, and interfacial strength of continuous bamboo fiber reinforced epoxy composites," *Composites Part B Engineering*, vol. 166, pp. 272–283, Dec. 2018, doi: 10.1016/j.compositesb.2018.12.013.

[16] W. Liu, T. Chen, X. Wen, R. Qiu, and X. Zhang, "Enhanced mechanical properties and water resistance of bamboo fiber–unsaturated polyester composites coupled by isocyanatoethyl methacrylate," *Wood Science and Technology*, vol. 48, no. 6, pp. 1241–1255, Sep. 2014, doi: 10.1007/s00226-014-0668-6.

[17] Z. Zhu, M. Hao, and N. Zhang, "Influence of contents of chemical compositions on the mechanical property of sisal fibers and sisal fibers reinforced PLA composites," *Journal of Natural Fibers*, vol. 17, no. 1, pp. 101–112, May 2018, doi: 10.1080/15440478.2018.1469452.

[18] R. Vishnuvardhan, R. R. Kothari, and S. Sivakumar, "Experimental investigation on mechanical properties of Sisal fiber reinforced epoxy composite," *Materials Today Proceedings*, vol. 18, pp. 4176–4181, Jan. 2019, doi: 10.1016/j.matpr.2019.07.362.

[19] Y. Li, Y.-W. Mai, and L. Ye, "Sisal fibre and its composites: a review of recent developments," *Composites Science and Technology*, vol. 60, no. 11, pp. 2037–2055, Aug. 2000, doi: 10.1016/s0266-3538(00)00101-9.

[20] A. Devaraju and P. Sivasamy, "Comparative Analysis of Mechanical Characteristics of Sisal Fibre Composite with and without Nano Particles," *Materials Today Proceedings*, vol. 5, no. 6, pp. 14362–14366, Jan. 2018, doi: 10.1016/j.matpr.2018.03.020.

[21] A. E. Bekele, H. G. Lemu, and M. G. Jiru, "Experimental study of physical, chemical and mechanical properties of enset and sisal fibers," *Polymer Testing*, vol. 106, p. 107453, Dec. 2021, doi: 10.1016/j.polymertesting.2021.107453.

[22] A. D. Gudayu, L. Steuernagel, D. Meiners, and R. Gideon, "Effect of surface treatment on moisture absorption, thermal, and mechanical properties of sisal fiber," *Journal of Industrial Textiles*, vol. 51, no. 2_suppl, pp. 2853S-2873S, May 2020, doi: 10.1177/1528083720924774.

[23] M. I. Khan and C. Nayak, "Finite element analysis and performance comparison of leaf spring based on unidirectional SISAL Fiber-Reinforced epoxy composite against woven Fiber-Reinforced composite," *Fibers and Polymers*, vol. 24, no. 9, pp. 3333–3343, Aug. 2023, doi: 10.1007/s12221-023-00303-8.

[24] A. A. M. Moshi, S. Madasamy, S. R. S. Bharathi, P. Periyanayaganathan, and A. Prabaharan, "Investigation on the mechanical properties of sisal – Banana hybridized natural fiber composites with distinct weight fractions," *AIP Conference Proceedings*, vol. 2128, p. 020029, Jan. 2019, doi: 10.1063/1.5117941.

[25] T. R. Prabhu, V. K. Varma, and S. Vedantam, "Effect of reinforcement type, size, and volume fraction on the tribological behavior of Fe matrix composites at high sliding speed conditions," *Wear*, vol. 309, no. 1–2, pp. 247–255, Nov. 2013, doi: 10.1016/j.wear.2013.10.001.

[26] K. Murugan, S. Venkatesh, R. Thirumalai, and S. Nandhakumar, "Fabrication and investigations of kenaf fiber and banana fiber reinforced composite material," *Materials Today Proceedings*, vol. 37, pp. 110–114, May 2020, doi: 10.1016/j.matpr.2020.04.540.

[27] K. Cho *et al.*, "Influence of surface treatment on the interfacial and mechanical properties of short S-Glass Fiber-Reinforced dental composites," *ACS Applied Materials & Interfaces*, vol. 11, no. 35, pp. 32328–32338, Aug. 2019, doi: 10.1021/acsami.9b01857.

[28] T. Padmavathi, S. V. Naidu, and R. Rao, "Studies on mechanical behavior of surface modified sisal fibre – epoxy composites," *Journal of Reinforced Plastics and Composites*, vol. 31, no. 8, pp. 519–532, Feb. 2012, doi: 10.1177/0731684412438954.

[29] M. R. Sanjay and B. Yogesha, "Studies on mechanical properties of Jute/E-Glass fiber reinforced epoxy hybrid composites," *Journal of Minerals and Materials Characterization and Engineering*, vol. 04, no. 01, pp. 15–25, Jan. 2016, doi: 10.4236/jmmce.2016.41002.

[30] F. G. Shin, X. -j. Xian, W. -p. Zheng, and M. W. Yipp, "Analyses of the mechanical properties and microstructure of bamboo-epoxy composites," *Journal of Materials Science*, vol. 24, no. 10, pp. 3483–3490, Oct. 1989, doi: 10.1007/bf02385729.

[31] M. K. Gupta and R. K. Srivastava, "Mechanical, thermal and dynamic mechanical analysis of jute fibre reinforced epoxy composite," *Indian Journal of Fibre & Textile Research*, vol. 42, no. 1, pp. 64–71, Mar. 2017.

[32] M. K. Gupta and R. K. Srivastava, "Properties of sisal fibre reinforced epoxy composite," *Indian Journal of Fibre & Textile Research (IJFTR)*, vol. 41, no. 3, pp. 235–241, Sep. 2016.

[33] S. Biswas, "Mechanical properties of bamboo-epoxy composites a structural application," *Advances in Materials Research*, vol. 1, no. 3, pp. 221–231, Sep. 2012, doi: 10.12989/amr.2012.1.3.221.

[34] R. H. Sadok *et al.*, "Mechanical Properties and Microstructure of Low Carbon Binders Manufactured from Calcined Canal Sediments and Ground Granulated Blast Furnace Slag (GGBS)," *Sustainability*, vol. 13, no. 16, p. 9057, Aug. 2021, doi: 10.3390/su13169057.

[35] R. Thirumalai, R. Prakash, R. Ragunath, and K. M. SenthilKumar, "Experimental investigation of mechanical properties of epoxy based composites," *Materials Research Express*, vol. 6, no. 7, p. 075309, Mar. 2019, doi: 10.1088/2053-1591/ab10f7.

[36] T. Ramanathan, K. Sithan, S. Ramanathan, and P. Ramasamy, "Parametric optimization in drilling process parameters for machining of glass fibre reinforced composites using Grey relational grade analysis," *Chiang Mai Journal of Science*, vol. 49, no. 5, Sep. 2022, doi: 10.12982/cmjs.2022.091.

[37] K. M. Senthil Kumar, S. Murugesan, V. Thangamuthu, T. Ramanathan, "Experimental investigation of palm kernel fibre reinforced epoxy based composite," *Journal of Ceramic Processing Research*, vol. 22, no. 6, pp. 731–738, Dec. 2021, doi: 10.36410/JCPR.2021.22.6.731.